



OPEN ACCESS

EDITED BY
Mariusz Cycoń,
Medical University of Silesia, Poland

REVIEWED BY
Muhammad Shahid,
University of the Punjab, Pakistan
Kandasamy Saravanakumar,
Kangwon National University,
South Korea

*CORRESPONDENCE
Zhiqing Wang
wangzhiqing@jlau.edu.cn

SPECIALTY SECTION
This article was submitted to
Microbiotechnology,
a section of the journal
Frontiers in Microbiology

RECEIVED 18 July 2022
ACCEPTED 08 September 2022
PUBLISHED 03 October 2022

CITATION
Wang Z, Wang Z, Lu B, Quan X,
Zhao G, Zhang Z, Liu W and Tian Y
(2022) Antagonistic potential
of Trichoderma as a biocontrol agent
against *Sclerotinia asari*.
Front. Microbiol. 13:997050.
doi: 10.3389/fmicb.2022.997050

COPYRIGHT
© 2022 Wang, Wang, Lu, Quan, Zhao,
Zhang, Liu and Tian. This is an
open-access article distributed under
the terms of the [Creative Commons
Attribution License \(CC BY\)](https://creativecommons.org/licenses/by/4.0/). The use,
distribution or reproduction in other
forums is permitted, provided the
original author(s) and the copyright
owner(s) are credited and that the
original publication in this journal is
cited, in accordance with accepted
academic practice. No use, distribution
or reproduction is permitted which
does not comply with these terms.

Antagonistic potential of Trichoderma as a biocontrol agent against *Sclerotinia asari*

Zhiqing Wang^{1*}, Ziqing Wang¹, Baohui Lu², Xingzhou Quan¹,
Guangyuan Zhao¹, Ze Zhang¹, Wanliang Liu¹ and Yixin Tian¹

¹College of Chinese Medicinal Materials, Jilin Agricultural University, Changchun, Jilin, China,
²College of Plant Protection, Jilin Agricultural University, Changchun, Jilin, China

In the present study, the inhibitory potential of 14 Trichoderma strains (isolated from Asarum rhizosphere) was investigated against *Sclerotinia asari* using the plate dilution method. The activity of antioxidant enzymes viz; catalase (CAT), peroxidase (POD), superoxide dismutase (SOD), and malondialdehyde (MDA) in *S. asari* treated with the two Trichoderma strains was also evaluated. Untargeted metabolomic analysis by using LC/MS analysis was carried out to determine differential metabolites in *T. hamatum* (A26) and *T. koningiopsis* (B30) groups. Moreover, transcriptome analysis of *S. asari* during the inhibition of *S. asari* by B30, and A26 compared with the control (CK) was performed. Results indicated that inhibition rates of *T. koningiopsis* B30, and *T. hamatum* A26 were highest compared to other strains. Similarly, non-volatile metabolites extracted from the B30 strain showed a 100% inhibition of *S. asari*. The activity of CAT, SOD, and POD decreased after treatment with A26 and B30 strains while increasing MDA content of *S. asari*. Antifungal activity of differential metabolites like abamectin, eplerenone, behenic acid, lauric acid, josamycin, erythromycin, and minocycline exhibited the highest inhibition of *S. asari*. Transcriptome analysis showed that differentially expressed genes were involved in many metabolic pathways which subsequently contributed toward antifungal activity of Trichoderma. These findings suggested that both Trichoderma strains (B30 and A26) could be effectively used as biocontrol agents against Sclerotinia disease of Asarum.

KEYWORDS

Trichoderma, *Sclerotinia asari*, biocontrol agent, antioxidant activity, metabolites, antifungal activity

Introduction

Plant diseases are one of the major factors that contribute directly to the depletion of agricultural natural resources (Benítez et al., 2004). These also contribute to 10–20% annual losses in global food production leading to a financial deficit of billions of dollars coupled with an adverse impact on food supply (Manczinger et al., 2002). Among plant

pathogens, fungi are the most virulent pathogens among the soil-borne infections that cause significant losses. Out of many fungal infections in plants, necrotrophic fungi *Sclerotinia* spp. are among the most virulent pathogenic fungi causing infection in a wide range of crops and plants (Bolton et al., 2006). *Sclerotinia* spp. spend around 90% of their entire cycle as sclerotia in the soil (Kim and Knudsen, 2008). Sclerotia germinate during specific periods of the year, based on the fungus's inherent potential and environmental factors, and create either mycelium or an apothecium to infect the host (Tyagi et al., 2020).

The *Sclerotinia* genus contains several species, each with a unique host organism on which it infects. *S. asari* is one of the members of the *Sclerotinia* fungal species that commonly infects Asarum (wild ginger) plants through its mycelium and causes Asarum sclerotiorum disease (Wang and Wu, 1983). *Asarum heterotropoides* Var. *Mandshuricum* is a popular perennial medicinal herb grown in the Liaoning Province of China and is commonly named Xixin (Huang et al., 2003). Essential oil isolated from *Asarum heterotropoides* Var. *Mandshuricum* possesses diverse therapeutic properties and is usually utilized as an analgesic, antibacterial, antifungal, and antitussive medicine in China (Perumalsamy et al., 2010). Previous studies have identified more than 82 compounds in the essential oil of Asarum with methyleugenol being the most prevalent compound (Zeng et al., 2004; Dan et al., 2010).

With the development of Asarum crops, Asarum sclerotiorum has emerged as a new concern. The disease was discovered in the Liaoning Province and Jilin Province in China (Wang and Wu, 1982). The *S. asari* has been found in both the underground and aerial sections of the affected plants. The disease causes rot in roots, seedlings, buds, stalks, and fruits eventually causing the entire plant to rot and die. Plant losses (that occur due to blighting) have been reported to be between 20 and 80% in cultivated gardens (Wang and Wu, 1984).

Various strategies including chemical and biological control methods are being employed to minimize the economic losses from plant pathogens like *S. Asari* infection. Chemical control methods have been effectively utilized to prevent plant diseases, but misuse has promoted the development of fungicide-resistant pathogens. Moreover, application of chemicals also destroys the ecological balance of soil microorganisms (Benítez et al., 2004; Kalia and Gosal, 2011). However, the development of genetic resistance against specific chemicals owing to genetic variations in populations also limits the potent effect of fungicides, whilst broad-spectrum fungicides also have adverse side effects on non-target species (Tjamos et al., 2013). Conventional chemical control approaches for many plant diseases may not always be cost-effective or efficient, and spraying and other chemical control methods might cause substantial health, safety, and environmental hazards (Monte, 2001). As a result, finding

healthy, safe, and efficient biological control techniques has become an important task for the pathogen-free crops. Biological control is safe for humans and animals and also ecologically sustainable due to its diverse sources (Ling et al., 2021).

Biological treatment of plant diseases is usually practiced by using antagonists of phytopathogenic fungi, and 90% of such treatments have utilized various strains of *Trichoderma* fungus (Benítez et al., 2004). Majority of *Trichoderma* strains do not have a sexual lifecycle but rather generate just asexual spores. Moreover, several *Trichoderma* species are anamorphically associated with *Hypocrea*, and their Internal Transcribed Spacer (ITS) sequences have confirmed their phylogenetic closeness (Monte, 2001). The genus *Trichoderma* works as a biocontrol agent because of its ability to combat infections. Many genes of *Trichoderma* with potential antifungal effects have been isolated, cloned, and examined to determine their mechanism and function for various activities such as cell wall disintegration, hyphal development, and antagonist activity against phytopathogens (Sharma et al., 2011).

Trichoderma spp. isolated from seed and soil have shown distinct antifungal effects against *Rhizoctonia solani*, which is a pathogenic fungus that causes root rot and reduces bean yield (Mayo-Prieto et al., 2020). Moreover, volatile metabolites released from *Trichoderma* spp. have shown to inhibit the growth of soil-borne phytopathogens. Hydrolases such as chitinase and glucanase are among many of the metabolites that are assumed to be directly associated with mycoparasitism. To breakdown the cell walls of phytopathogen, the antagonistic *Trichoderma* synthesizes extracellular hydrolases which directly attack pathogens (Küçük and Kivanç, 2005). Recently, Ling et al. (2021) identified a strain of *Monosporascus ibericus* (AR-4-1) with the most potent antifungal effect against *S. asari* through the plate confrontation method from a collection of 31 strains having antagonistic effects on plant pests (Ling et al., 2021).

Previous studies have shown antagonistic potential of *Trichoderma* spp. against different phytopathogens by releasing metabolites and inhibiting their growth, however, the inhibitory potential of *Trichoderma* spp. against *S. asari* needs to be studied thoroughly because this phytopathogen is fatal for certain Asarum plants and can cause serious economic losses. Therefore, in the present study, the antifungal action of volatile and non-volatile compounds of two *Trichoderma* strains was tested against the *S. asari*. Metagenomic and metabolomic analysis was performed to investigate the antagonistic effect of volatile and non-volatile compounds of *Trichoderma* strains against the *S. asari* causing rot in *Asarum heterotropoides* Var. *Mandshuricum* plant. It was hypothesized that *Trichoderma* strains can be utilized as a biological control agent against the invading pathogen owing to its active metabolites to protect the Asarum crop.

Materials and methods

Isolation of *Trichoderma* strains and *Sclerotinia asari*

Trichoderma strains were isolated from the rhizosphere soil of healthy *Asarum heterotropoides* var. *mandshuricum* plants by the soil dilution method as described previously (Gil et al., 2009). Ten samples of the rhizosphere soil of healthy *Asarum* plants in Tonghua (E125°34', N41°78') and Liuhe cities (E125°75', N42°24', Jilin Province) were collected. Five-fold serial dilutions of every sample were made and 0.5 ml of the diluted sample containing *Trichoderma* spp. was poured on top of culture medium for culturing. Briefly, using the plate dilution method, 10 g of soil samples were added to 90 mL of sterile water, and mixed well. About 1 mL of this suspension was added into 9 mL of sterile water to make 10% soil suspension, and then diluted it with sterile water to 10⁻³ and spread it on the PDA medium. Mycelium at the edge of the colony was picked after cultivating for 3d with inversion culture at 28°C, and then inoculated it into a new PDA medium. Purified colonies were obtained after repeating above steps 5–6 times, and stored at 4°C for later use. Target fungus of *S. asari* was also isolated from the infected *Asarum* plants. The samples were carried to the lab and kept at 4°C until further processed.

Molecular and morphological identification of *Trichoderma* isolates

The *Trichoderma* strains were inoculated into a PD liquid medium and placed in the culture plate in a shaking incubator for 5 days at 25°C. After that, the cells were centrifuged and freeze-dried at -80°C for 2–3 days before grinding into powder. The genomic DNA from *Trichoderma* culture was extracted as described previously (Möller et al., 1992). Two sets of double primers (nested primers) including one ITS primer ITS4 (5'-TCCTCCGCTTATTGATATGC-3') and ITS1 (5'-TCCGTAGGTGAACCTGCGG-3') was used to amplify a 600 bp fragment of ITS region of the ribosomal DNA (rDNA) gene. The PCR amplification conditions for this reaction were: pre-denaturation at 94°C for 5 min; 35 cycles of denaturation at 94°C for 30 s, annealing at 48°C for 40 s, extension at 72°C for 1 min; and renaturation at 72°C for 10 min. The second set of primer was rRPB2-5F (5'-GAYGAYMGWGATCAYTTYGG-3'), rRPB2-7cR (5'-CCCATRGCTTGYTTRCCCAT-3') that was used to amplify a 1,000 bp fragment of the second largest RNA polymerase subunit gene (RPB2 gene) and identify the target fungi (White et al., 1990). The PCR conditions for this amplification reaction were: pre-denaturation at 95°C for 5 min; denaturation at 95°C for 1 min, annealing at 55°C for 90 s, extension at 72°C for 90 s, 35 cycles; and final amplification at

72°C for 7 min. The obtained ITS sequences of the *Trichoderma* strains were compared to the related sequences in the GenBank database. Based on ITS-RPB2 double sequence alignment, phylogenetic tree of *Trichoderma* was constructed by using neighbor-joining method using MEGA11 software (Tamura et al., 2021). For morphological identification, *Trichoderma* strains were cultured on PDA and Oatmeal agar (OA) medium (30 g oat flakes, 13 g agar, per L of distilled water, pH 6.5) and characteristics of conidiophores were observed under high resolution compound microscope.

Screening of *Trichoderma* strains for antagonistic activity

Determination of antagonistic effect of *Trichoderma* strains against *Sclerotinia sclerotiorum*

The activated *Sclerotinia sclerotiorum* cake (with a diameter of about 0.5 cm) was inoculated on the PDA medium. The fungal cake was put 2 cm away from the center of the medium and cultured at 25°C for 36 h. On the other side, a fresh *Trichoderma* strain cake, and the fungus cake was equidistant from the edge of the petri dish, and the control (without *Trichoderma*) was used as the blank. Each treatment was repeated three times. After 7 days, the diameter was measured by the cross method and the fungistatic rate was calculated using the following formula;

$$\text{Fungistatic rate} = \frac{\text{Diameter of control colonies} - \text{Diameter of treated colonies}}{\text{Diameter of control colonies}} \times 100\%$$

Determination of the antagonistic effect of *Trichoderma* volatile substances on *Sclerotinia sclerotiorum*

The *Trichoderma* fungus cake was inoculated in the center of the PDA flat plate, and the bottom of another PDA flat plate was used to replace the top of the flat plate. After culturing at 25°C for 5 d, the diameter was measured by the cross method and the fungistatic rate was calculated using the above mentioned formula.

Determination of the antagonistic effect of non-volatile substances of *Trichoderma* on *Asarum sclerotiorum*

Sterile double cellophane on the PDA medium was spreaded, inoculated *Trichoderma* fungus cake in the center of the plate, and removed the cellophane with sterile tweezers when the mycelium grew to the edge of the cellophane. Then, the center of the plate was inoculated with *Asarum sclerotiorum* cake, and no *Trichoderma* was used in the control sample, and each treatment was repeated three times.

Extraction of metabolites

After initial screening, non-volatile metabolites of two *Trichoderma* strains (*T. hamatum* A26 and *T. koningiopsis* B30) were extracted by ethyl acetate and water-saturated n-butyl alcohol. Fermentation broths of *T. hamatum* A26 and *T. koningiopsis* B30 were filtered and extracted with an equal volume of ethyl acetate. Both extracts were separately dried under vacuum at 40°C. After that, these extracts were dissolved in methanol, and the metabolite components of the extracts were identified by LC-MS analysis (Blaženović et al., 2018; Zeki et al., 2020).

LC-MS conditions for differential metabolite analysis

A 20 μ L of internal standard (L-2-chlorophenylalanine, 0.3 mg/mL; methanol configuration) was added to the samples (vortexed for 30 s, and sonicated for 3 min); and centrifuged for 10 min (at 13,000 rpm, 4°C). After that 150 μ L of supernatant was removed with a syringe, filtered through a 0.22 μ m organic phase pinhole filter, and then transferred to LC injection vials. It was then stored at -80°C until LC-MS analysis was performed.

Liquid-mass spectrometry system (AB SCIEX ExionLC 2.0+system, USA) containing ultra-high-performance liquid phase series (QE) high-resolution mass spectrometer was used to analyze the metabolome of two antagonist *Trichoderma* strains. Conditions for the liquid phase and mass spectrometry are given in Tables 1, 2.

Determination of antioxidant activity

The activity of CAT, POD, SOD, and MDA enzymes of *S. asari* treated with *Trichoderma* strains was analyzed using the commercial kits following manufacturer's instructions (Beyotime Biotechnology, Shanghai, China). Samples of treated *S. asari* were homogenized in 5 ml of 50 mM sodium phosphate buffer (pH 7.00). The homogenized sample was

filtered before being centrifuged at 13,000 g for 20 min in a chilled centrifuge, and supernatant was used for further analysis. All procedures were carried out at 4°C according to recommended instructions for each analytical kit (Beyotime Biotechnology, Shanghai, China).

Ribonucleic acid isolation, cDNA library preparation, and Illumina sequencing

For transcriptome analysis, firstly, the total RNA of 12 samples (four from each treatments A26, B30, and control group) was isolated according to the manufacturer's instructions using the Qiagen RNeasy Plant Mini Kit (QIAGEN, Germany). Using a spectrophotometer (NanoDrop ND-1000; Thermo Fisher Scientific, Waltham, MA, USA), the quantity and quality of the RNA samples were determined. The TruSeq[®] RNA Sample Preparation Guide from Illumina¹ was used to create the fragment libraries. The Standard Cluster Development kit from Illumina was then used to load these libraries into the cluster generation station for single-molecule bridge multiplication. The Illumina Genome Analyzer I (GAI) was used to sequence the slide containing amplified clusters for single reads through using Illumina 36 cycle Sequencing Kit version 1. The Illumina Hi-Seq high-throughput sequencing platform sequences the cDNA library using Sequencing By Synthesis (SBS) technology, and the image data acquired using the high-throughput sequencer is transformed into a huge number of high-quality Data, known as raw data, by CASAVA base recognition (Caporaso et al., 2012).

Transcriptome assembly and analysis

Raw sequencing reads with a quality score of less than 20 (\geq Q20) were eliminated using the cutadapt tool (Martin, 2011) and filtered to get clean reads. To screen clean reads, the FastQC v0.11.7 visualization program was utilized based on several parameters including, per-sequence quality score, GC content, error distribution, K-mer content, and sequence length distribution. Trinity was utilized in the project to join the clean reads. The contigs were clustered using the TGICL and Phrap programs to further combine the sequences and avoid any duplication at 90% sequence homology (Shentu et al., 2014). The Trinity Perl script was used to generate unigenes. The CD-HIT was used to integrate and cluster A26, B30, and CK clustered assemblies to build a A26_CK and B30_CK combined assembly. From these merged assemblies, unigenes were recovered. All samples were mapped against A26_CK

TABLE 1 Liquid phase conditions for LC-MS analysis.

Parameters	Description
Column	ACQUITY UPLC HSS T3 (100 mm \times 2.1 mm, 1.8 μ m)
Column temperature	45°C
Mobile phase	A-water (containing 0.1% formic acid) B-acetonitrile (containing 0.1% formic acid)
Flow rate	0.35 mL/min
Injection volume	2 μ L

¹ <http://www.illumina.com>

and B30_CK unigenes with standard settings using the BWA-MEM tool (version 0.7.5). The final transcripts were utilized for downstream analysis.

Gene functional annotation and differential analysis

The assembled reads were used to measure gene expression, and the transcripts were accurately determined by using Cufflinks program. The quantification of each gene was measured in the form of fragments per kilobase of exon per million mapped reads (FPKM) by using RSEM tool (Li and Dewey, 2011). Differential analysis of all possible samples' combination was carried out by utilizing DESeq 2 (V 1.6.3) by using default parameters like p -values and log₂FC. The unigene sequence was compared with GO, NT, NR, Swiss-Prot, KO, and KOG, databases using Blast2GO software V 3.0 (Conesa et al., 2005). After predicting the amino acid sequence of unigenes, the HMMER software (Finn et al., 2011), was used to search the Pfam database to obtain the annotation information of unigenes. Moreover, pathway analysis was performed on the predicted proteins using the Kyoto Encyclopedia of Genes and Genomes (KEGG). Using default parameters, the identified proteins were divided into five functional groups: biological processes, metabolic processes, Genetic Information Processing, cellular processes, and environmental Information Processing. The KEGG database was used to find metabolic pathways associated with important DEGs.

Statistical analysis

All experimental results are presented as mean \pm standard deviation. Analysis of variance (ANOVA) under completely randomized design was used to analyze the effect of treatments. Statistical significance was declared at $P < 0.05$. Statistical tools like R program were used for the statistical analysis of metabolome and transcriptomic data. Differential metabolites across samples were identified using $VIP \geq 1$ and absolute Log₂FC (fold change) ≥ 1 .

Results

Morphological and molecular identification of *Trichoderma* isolates

Trichoderma isolates were identified by culturing *Trichoderma* strains on PDA and OA medium. Six species were identified including, *Trichoderma harzianum*, *Trichoderma hamatum*, *Trichoderma koningiopsis*, *Trichoderma*

TABLE 2 Mass spectrometry conditions.

Parameter	Positive ions	Negative ion
Mass scan range	100–1,200	100–1,200
Resolution (full scan)	70,000	70,000
Resolution (HCD MS/MS scans)	17,500	17,500
Spray voltage (V)	3,800	–3,200
Sheath gas flow rate (Arb)	40	40
Aux gas flow rate (Arb)	10	10
Capillary temperature (°C)	350	350

atroviridae, *Trichoderma brevicompactum*, and *Trichoderma tomentosum*. Morphology of *Trichoderma* strains on two different mediums and the conidiophores were visualized under high resolution microscope (Figure 1). *Trichoderma* strain B30 showed dense green conidiophores at the center of the plate under PDA medium while it was concentrated on the borders in OA medium. The A26 strain showed dispersed conidiophores at the borders in PDA (Figure 1).

The objective of phylogenetic studies was to identify the isolates' position and relationship with the known species of *Trichoderma*. In the phylogenetic tree, *T. koningiopsis*, *T. atroviridae*, and *T. hamatum* were belonged to the same clade and distinguished with bootstrap value of 99%. Similarly, *T. brevicompactum*, *T. tomentosum*, and *T. harzianum* were belonged to the same clade (Figure 2).

Antagonistic activity of *Trichoderma* strains against *Sclerotinia asari*

A total of 14 *Trichoderma* strains were isolated from the rhizosphere of *Asarum heterotropoides* var. *mandshuricum* plant. *Trichoderma* isolates showed rapid growth on PDA than pathogenic fungi *S. asari* under the same growth conditions. Results revealed that different isolates of *Trichoderma* inhibited the growth of phytopathogenic fungus *S. asari* to a varying extent (Table 3). However, highest inhibition rate was observed for two *Trichoderma* strains including A26 (92.77%), and B30 (91.32%). Whilst the lowest inhibition rate was shown by the D3 strain of *T. brevicompactum* (57.84%). The mycelial growth of the pathogenic fungi was suppressed substantially in the presence of an antagonist (*Trichoderma* strain) as compared to the control sample (Figure 3). All 14 *Trichoderma* strains exhibited different degrees of inhibition on the *Asarum sclerotiorum*. After 3rd days, both fungi came in contact each other and *S. asari* fungus stopped growing. In the presence of strains A26, F1, and B30, the mycelial growth of the *S. asari* was reduced significantly (Figure 3 and Table 3).

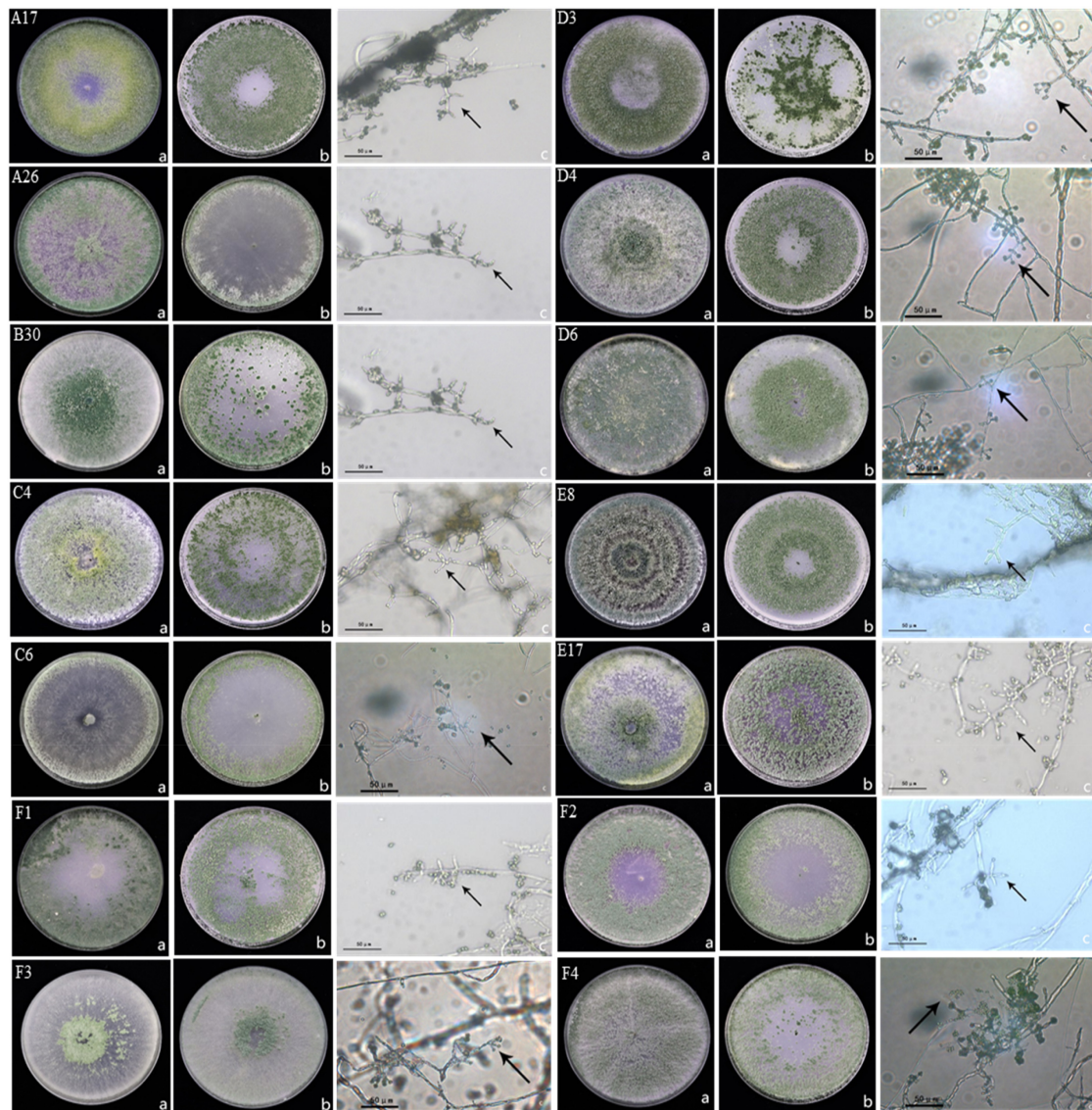


FIGURE 1

Morphology of *Trichoderma* strains (A) morphology of *Trichoderma* strains in PDA medium at 7d, (B) morphology of *Trichoderma* strains in OA medium at 7d, and (C) characteristics of conidiophore under a 40 × microscope; A17, C4, D4, D6, and E8 were classified as *Trichoderma harzianum*; B30, F1, and F2 were classified as *Trichoderma koningiopsis*; A26, C6, and F4 were classified as *Trichoderma hamatum*; E17 was classified as *Trichoderma atroviride*; D3 was classified as *Trichoderma brevicompactum*, F3 was classified as *Trichoderma tomentosum*.

Effect of volatile and non-volatile metabolites of *Trichoderma* on the growth of *Sclerotinia asari*

Both volatile and non-volatile compounds of *Trichoderma* strains were extracted to evaluate their antifungal activity against the phytopathogen *S. asari* through in-vitro assay. All of the *Trichoderma* isolates synthesized harmful volatile compounds that had a substantial influence on the radial outgrowth of the *S. asari* (Table 4). The volatile metabolites of *T. hamatum* (C6) were more effective against *S. asari* as these compounds reduced

mycelial growth up to 53.73%, followed by *T. koningiopsis* (B30) and *T. brevicompactum* (D3) strains with 45.77 and 37.61 percent inhibition, respectively. However, volatile metabolites from the *T. hamatum* (C4) strain showed the lowest inhibition rate (14.93%).

Non-volatile compounds isolated from the *T. koningiopsis* (B30) strain showed 100% inhibition of the phytopathogen *S. asari*, followed by *T. hamatum* A26 (86.67%) and C6 (84.44%) strains (Table 5). The bacteriostatic rate of non-volatile substances of A17 and D3 strains was higher than 75%.

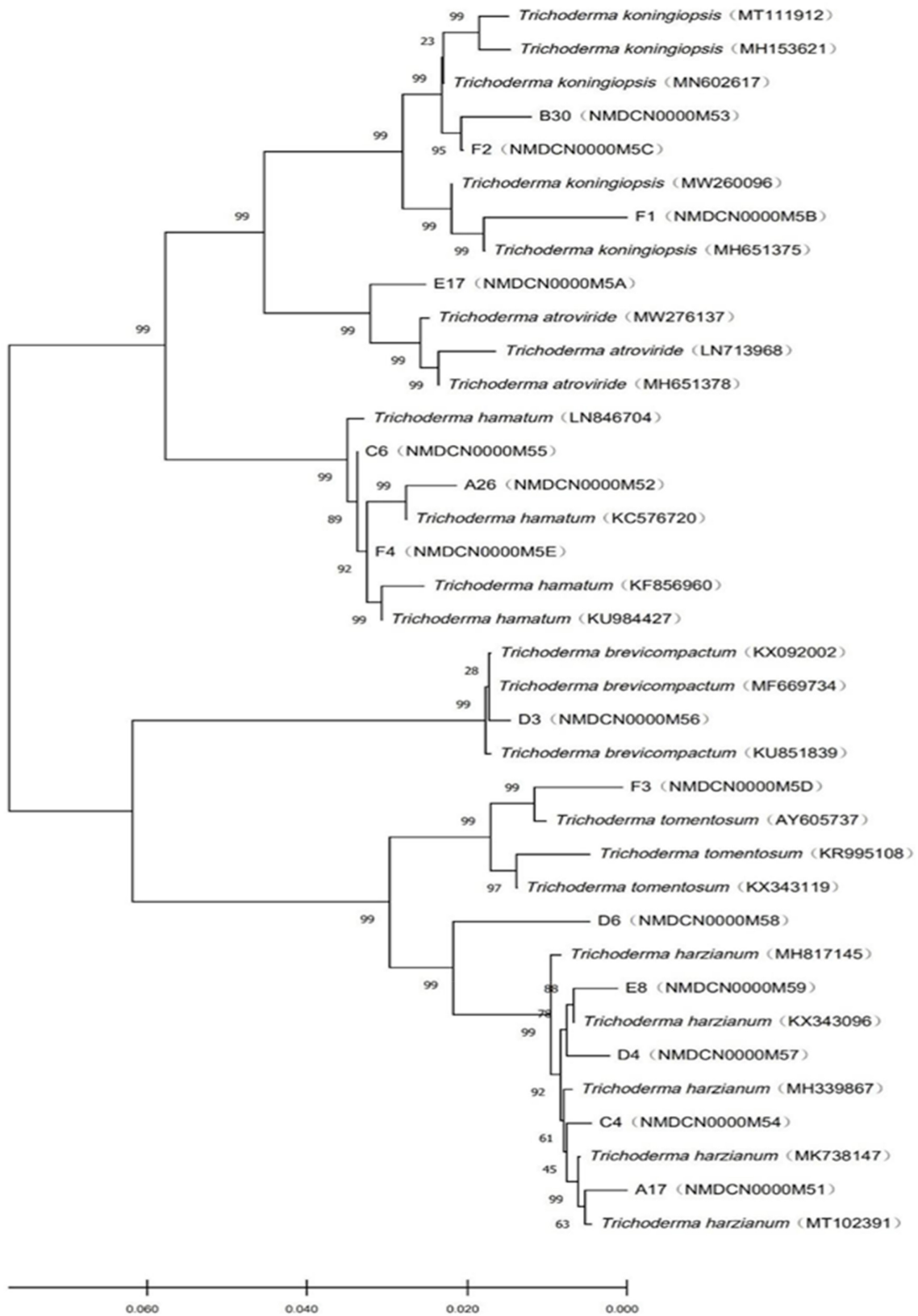


FIGURE 2
Phylogenetic tree of *Trichoderma* constructed based on the ITS-RPB2 double sequence alignment.

TABLE 3 Inhibition rate of different *Trichoderma* strains against *Sclerotinia asari*.

Strains number	Inhibition rate (%)	Strains number	Inhibition rate (%)
A17	90.16 ± 0.02 ^a	D6	79.34 ± 0.04 ^b
A26	92.77 ± 0.00 ^a	E8	89.26 ± 0.01 ^a
B30	91.32 ± 0.01 ^a	E17	88.06 ± 0.01 ^a
C4	73.63 ± 0.01 ^{bc}	F1	72.48 ± 0.01 ^{cd}
C6	90.83 ± 0.01 ^a	F2	76.86 ± 0.01 ^{bc}
D3	57.84 ± 0.02 ^f	F3	71.32 ± 0.00 ^{cd}
D4	64.46 ± 0.05 ^c	F4	67.35 ± 0.02 ^{de}

Values with different lowercase letters indicate significant differences ($P < 0.05$).

Metabolites of n-butyl alcohol extract

Based confrontation assay, two *Trichoderma* strains (A26 and B30) showing highest inhibition rate was selected for differential screening of metabolites through LC/MS analysis.

Screening of differential metabolites

A total of 4,124 metabolites were identified through LC/MS analysis out of which 1,096 were negative ions metabolites 3,028 were positive ions (Figure 4). The positive and negative ion data were combined into a data matrix table containing all the information extracted from the original data and used for subsequent analysis. Out of total identified metabolites, 517 differential metabolites were screened having a valid ID. Out of all these identified antifungal substances, the top 50 differential metabolites from both strains are presented on the heatmap cluster diagram (Figure 5). Metabolites shown in red have a maximum

score in each strain. Out of 50, about 15 metabolites were abundant in B30 strain including Cortisol, PE [14:0/22:2(13Z, 16Z)], Josamycin, Validamycin A, Methoxamine, Spiramycin, and phytosphingosine. In A26 strain, 35 metabolites were most abundant with the highest score including Nialenol, Zapoerin, Ergosterol, Monotropein, Minocyclin, Benazepril etc. Correlation cluster diagram was constructed to present the most abundant differential metabolites in both A26 and B30 strains (Figure 6). From the data, we have screened and narrowed down further to identify top 14 most effective and abundant antifungal substances from both strains, based on the relative abundance (peak value $\geq 10,000$) against *S. asari* (Table 6).

Antifungal activity test of differential metabolites against *Sclerotinia asari*

Antifungal activity of the top 14 differential metabolites against pathogenic fungus *S. asari* was examined using the dilution method. All compounds exhibited antifungal activity against *S. asari* with varying degrees. Based on the clear zone diameter, Abamectin, Behenic acid, Eplerenone, Erythromycin, Josamycin, Methylugenol, and Minocycline compounds showed higher antifungal activity (Figure 7).

Kyoto encyclopedia of genes and genomes classification and enrichment analysis

All differential metabolites were mapped through the KEGG (Kyoto Encyclopedia of Genes and Genomes) database. The KEGG classification and enrichment analysis showed that differential metabolites of *Trichoderma* are involved in many metabolic pathways like Tyrosine metabolism, Phenylalanine metabolism, pyrimidine metabolism, and galactose metabolism etc. Top 20 metabolic pathways were collected in which

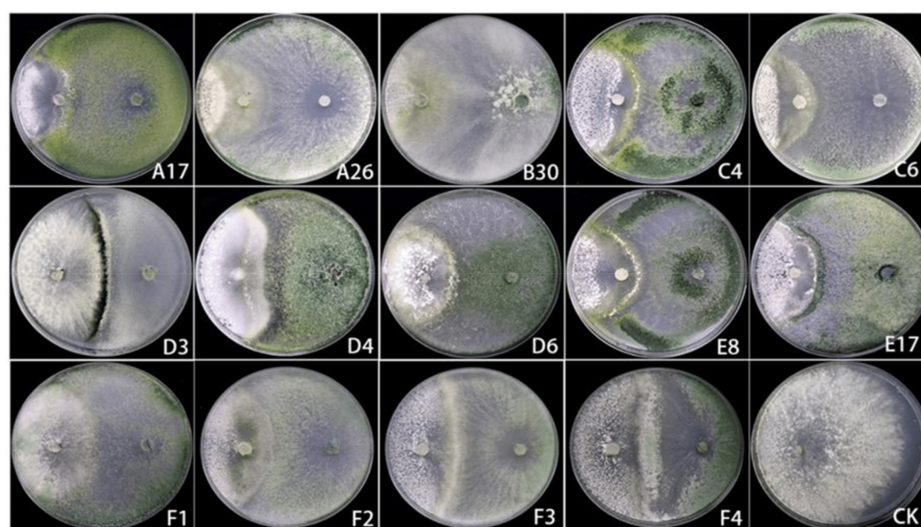


FIGURE 3
The confrontation effect of *Trichoderma* strains against *Sclerotinia asari*.

TABLE 4 Inhibition rate of volatile metabolites of *Trichoderma* strains against *Sclerotinia asari* ($\bar{x} \pm s$, $n = 3$).

Strain	Inhibition rate %	Strain	Inhibition rate %
A17	25.07 ± 0.03 ^{efg}	D6	28.16 ± 0.02 ^{ef}
A26	35.52 ± 0.01 ^{cd}	E8	35.12 ± 0.04 ^{cd}
B30	45.77 ± 0.06 ^b	E17	29.35 ± 0.00 ^{def}
C4	14.93 ± 0.03 ^h	F1	22.99 ± 0.00 ^{fg}
C6	53.73 ± 0.07 ^a	F2	15.32 ± 0.02 ^h
D3	37.61 ± 0.05 ^c	F3	19.80 ± 0.05 ^{gh}
D4	31.64 ± 0.02 ^{cde}	F4	30.85 ± 0.02 ^{de}

Values with different superscripts in same column differ significantly ($P < 0.05$).

TABLE 5 Inhibition rate of non-volatile metabolites of *Trichoderma* strains against *Sclerotinia asari*.

Strain	Inhibition rate (%)	Strain	Inhibition rate (%)
A17	78.67 ± 0.01 ^{bc}	D6	34.22 ± 0.03 ^f
A26	86.67 ± 0.01 ^b	E8	42.67 ± 0.11 ^{ef}
B30	100.00 ± 0.00 ^a	E17	40.44 ± 0.01 ^{ef}
C4	45.78 ± 0.08 ^c	F1	74.67 ± 0.04 ^c
C6	84.44 ± 0.04 ^{bc}	F2	64.44 ± 0.03 ^d
D3	76.00 ± 0.01 ^c	F3	58.22 ± 0.03 ^d
D4	37.33 ± 0.04 ^{ef}	F4	63.11 ± 0.03 ^d

Values with different superscripts in same column differ significantly ($P < 0.05$).

the amino acid metabolism (Tyrosine, phenylalanine, and Tryptophan metabolism) pathway possessed the highest number of metabolites, richness factor just less than 0.3, and P -value < 0.005 ([Supplementary Table 7](#)).

Determination of malondialdehyde content and antioxidant activity

The *S. asari* treated with *Trichoderma* strains showed higher MDA content ([Supplementary Table 1](#)). The average MDA content of *S. asari* treated with replicates of A26, B30, and D6 strains of *Trichoderma* were 1.12 ± 0.02 , 0.57 ± 0.10 , and 0.52 ± 0.07 ($\mu\text{mol/g}$) respectively, were highest among other groups. The MDA content of *S. asari* after A26 treatment was 7.7 times greater than that of the control group. The MDA content of other treatment groups was significantly higher than the control group ($P < 0.05$).

After treatment with *Trichoderma* strains, the activity of antioxidative enzymes was decreased significantly in *S. asari*. The activity of SOD in *S. asari* was reduced significantly after treatment with *Trichoderma* strains D6 ($15.49 \pm 0.6^\circ\mu\text{g.min}$), D3 (21.89 ± 0.3 U/g.min), and C6 (25.92 ± 0.4 U/g.min) compared to control group (85.28 ± 3.1 U/g.min) ([Supplementary Table 2](#)).

Similarly, CAT activity was reduced significantly after treatment with *Trichoderma* strains E17, B30, and A26 (7.4 ± 1.3 , 8.6 ± 0.4 , and 16.2 ± 0.6 U/g.min, respectively), as compared to the control group (35.6 ± 0.7 U/g.min). The CAT activity of *S. asari* was reduced by 75.84% after treatment with B30 strain, which was significantly lower ($P < 0.05$) than other treatment groups ([Supplementary Table 3](#)). POD activity of *S. asari* treated with C6 was (8.33 U/g.min) decreased by 67.86% as compared to the control group (25.92 ± 3.20 U/g.min) ([Supplementary Table 4](#)).

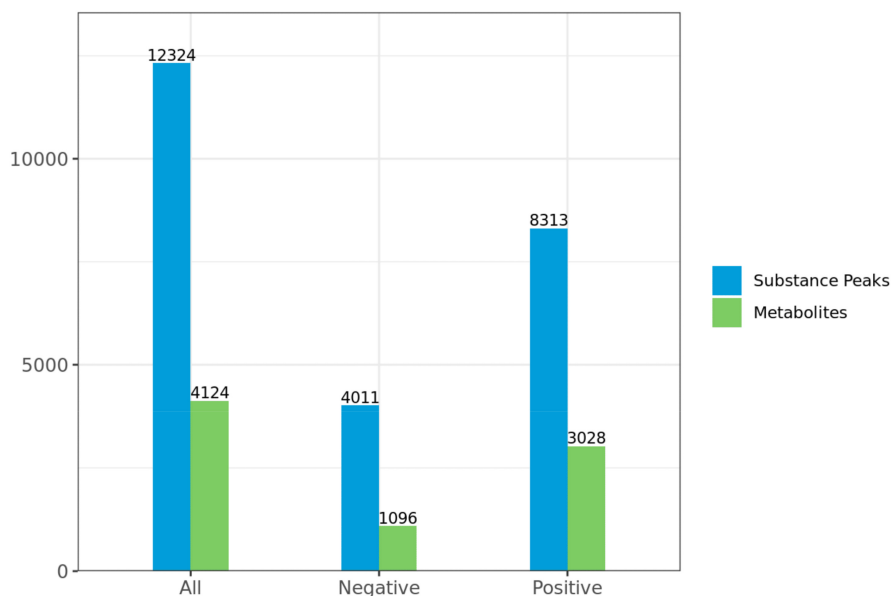
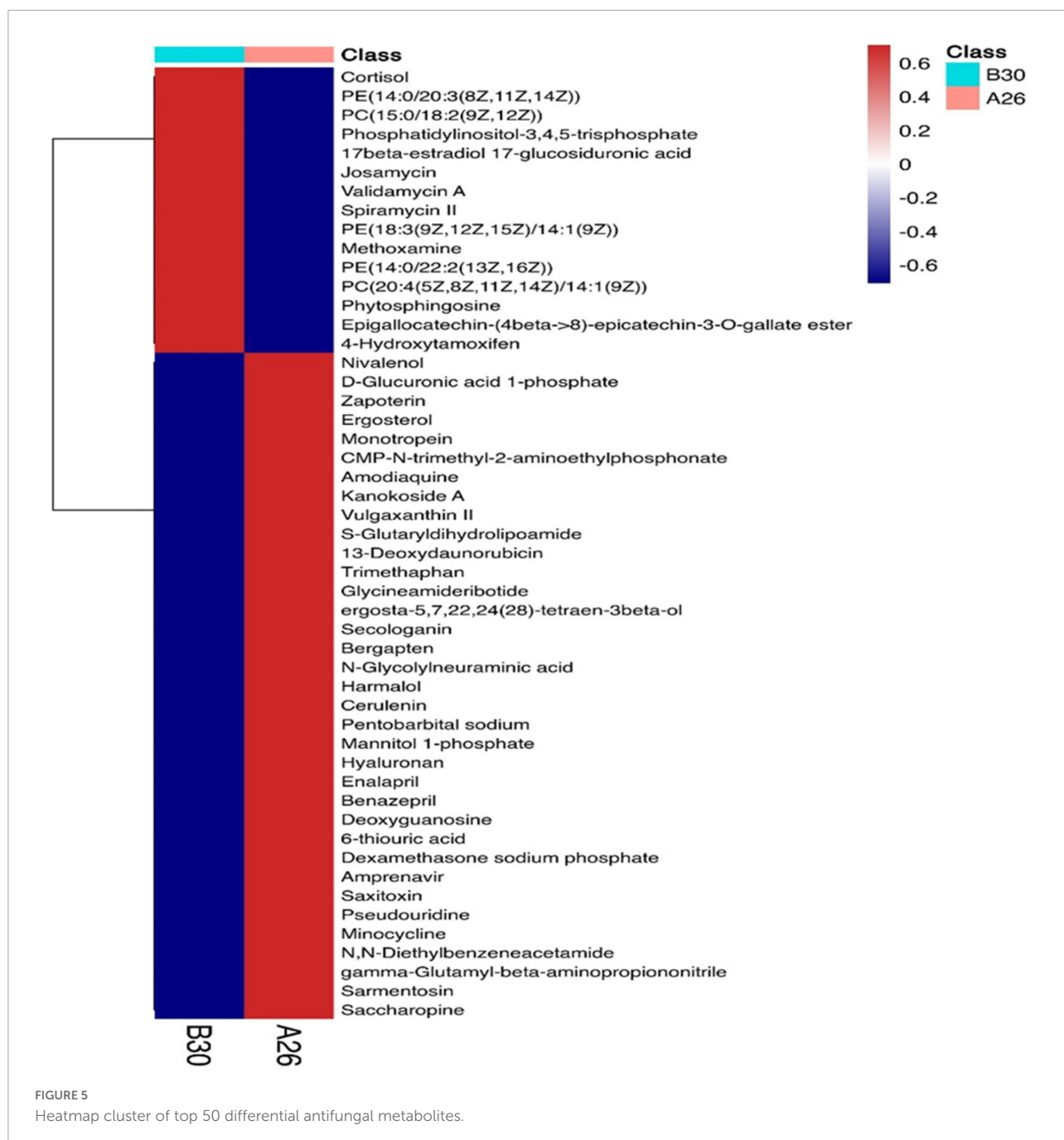


FIGURE 4
Statistics of substance peaks and metabolites.



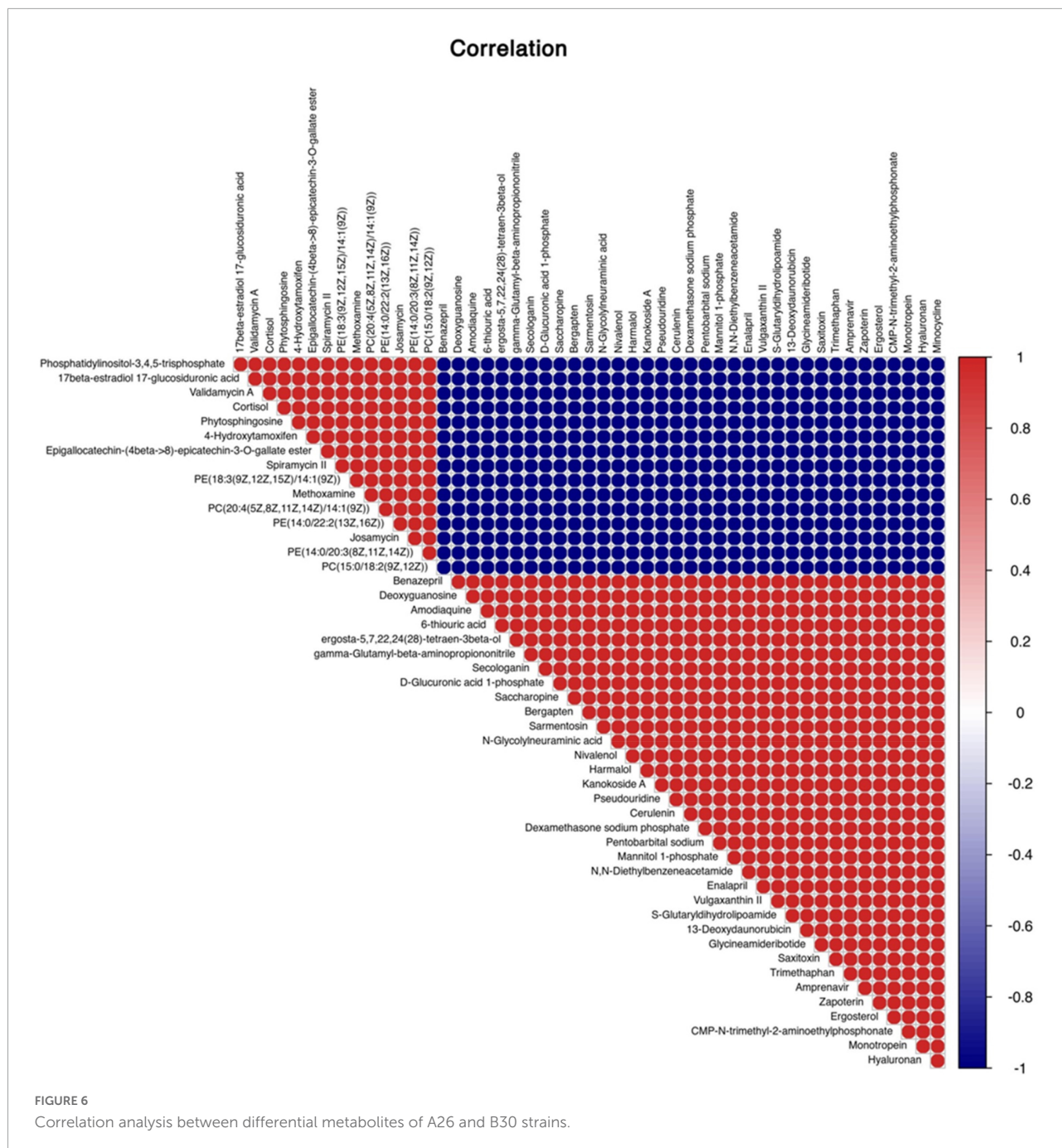
Illumina sequencing quality control and sequence assembly

Sequence data screening and assembly

The sequencing data obtained from strain B30 contains 97.33% proportion of clean reads, while A26 strains contain 98.39% of clean reads as compared to the control group CK1. The composition of filtered sequencing data of each sample is shown in [Supplementary Figure 1](#). The error rate distribution plot of the sequencing data of

each sample can be seen in [Supplementary Figure 2](#). GC content along base reads obtained from B30 strain is 47.5% while it is 52.68% in A26 strain as compared to the CK1 GC content which is 46.09%. The GC content distribution map of each sample can be seen in the ([Supplementary Figure 3](#)).

The clean reads utilized in the following study are obtained after raw data filtering, sequencing error rate checking, and GC content distribution checking, and the data summary is provided in [Supplementary Table 5](#).



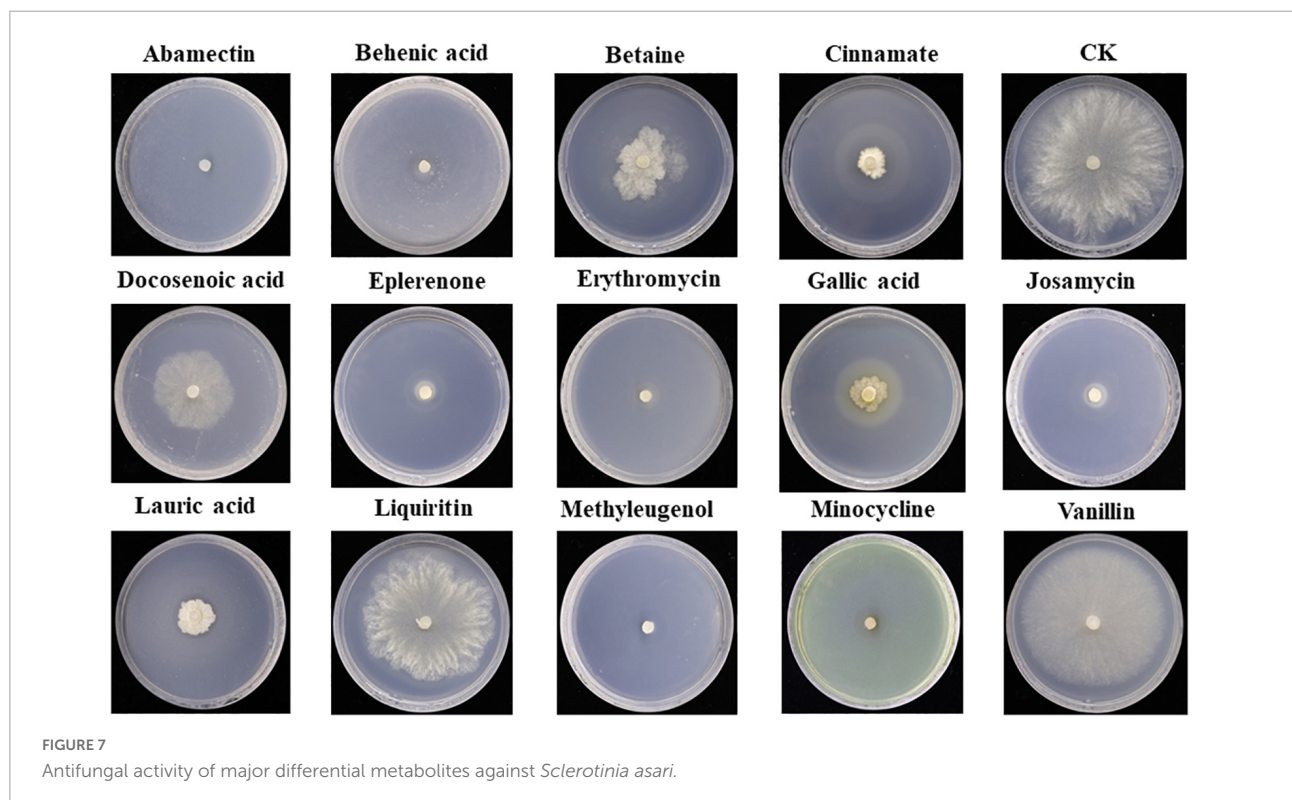
After obtaining clean reads for projects with no reference genome, the clean reads must be spliced to produce reference sequences for later analysis. Trinity software generated a total 301,490,876 bp nucleotides with a mean contig length of 1697 bp, N50 of 2896 bp, and N90 of 690 bp. A total of 100,118 unigenes were generated with a mean length of 1,365 bp and N50 of 2,319 bp. The size distribution of these unigenes and transcripts length interval is shown in [Supplementary Figure 4](#).

Gene function annotation

The Unigene sequences were compared with GO, NT, NR, Swiss-Prot, KO, and KOG, databases using BLAST, and after predicting the amino acid sequence of Unigene, the HMMER software was used to compare with Pfam database to obtain the annotation information of Unigene. Annotation of unigenes in seven databases was performed ([Supplementary Figure 5](#)) and the KEGG classification of genes involved

TABLE 6 Chemical formula, retention time, classification information, and peak values of chemicals.

Metabolites	Retention time (min)	Super class	Formula	Mass error (ppm)	A26	B30
Eplerenone	10.2305	Lipids and lipid-like molecules	C ₂₄ H ₃₀ O ₆	-0.6162	5700417	5780019
Lauric acid	5.81235	Lipids and lipid-like molecules	C ₁₂ H ₂₄ O ₂	-0.44073	432089.8	724646.6
Behenic acid	10.83105	Lipids and lipid-like molecules	C ₂₂ H ₄₄ O ₂	-1.03304	1163034	636872.5
13Z,16Z-docosadienoic acid	15.69548	Lipids and lipid-like molecules	C ₂₂ H ₄₀ O ₂	-0.99472	223124.6	284071.3
Erythromycin C	13.55027	Organoheterocyclic compounds	C ₃₆ H ₆₅ NO ₁₃	1.637536	110266.8	219868
Josamycin	9.583817	Organic oxygen compounds	C ₄₂ H ₆₉ NO ₁₅	1.928782	0.000154	112371.3
Methyleugenol	4.6542	Benzenoids	C ₁₁ H ₁₄ O ₂	-0.45125	408.6141	38657.85
Epigallocatechin gallate	13.83662	Phenylpropanoids and polyketides	C ₂₂ H ₁₈ O ₁₁	-5.38426	440.3525	14620.66
Betaine	1.9765	Organic acids and derivatives	C ₅ H ₁₁ NO ₂	1.780473	35037.89	14607.93
2-Hydroxycinnamic acid	2.181733	Phenylpropanoids and polyketides	C ₉ H ₈ O ₃	-0.35413	165365.7	11617
Vanillin	4.073883	Benzenoids	C ₈ H ₈ O ₃	-0.48565	11015.62	3260.618
(2S)-Liquiritigenin	2.502067	Phenylpropanoids and polyketides	C ₁₅ H ₁₂ O ₄	-9.60528	52322.67	179.2478
Minocycline	5.250367	Phenylpropanoids and polyketides	C ₂₃ H ₂₇ N ₃ O ₇	-2.73946	357687.4	0.000154
Avermectin	7.615217	Lipids and lipid-like molecules	C ₄₉ H ₇₄ O ₁₄	4.191199	44323.75	11993.04

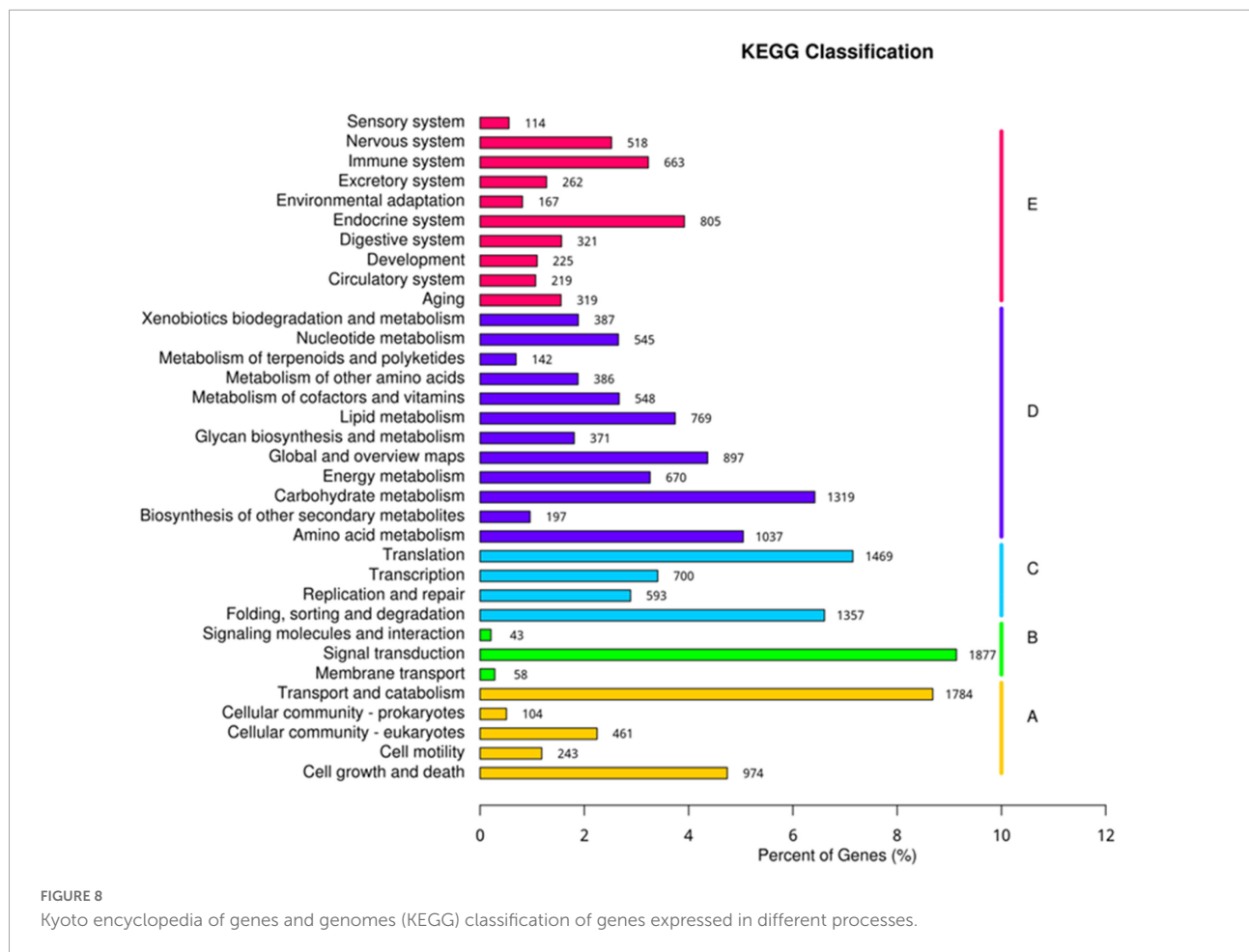


in different processes was determined (Figure 8). Biological processes, metabolic processes, genetic information processing, environmental information processing, and cellular processes were the top processes involving highest number of genes. The present study identified 805 genes involved in the endocrine system, 1,319 genes in carbohydrate metabolism, 1,469 genes in the translation process, 1,877 genes in signal transduction, and 1,784 genes in the transport and catabolism processes (Figure 8).

Genes quantification

Total gene count and distribution of all transcripts in each sample

Total reads of each sample were mapped to check the quantity of gene expression. The percentage of mapped genes from total reads was above 82% for every sample (Supplementary Table 6). For the calculation of the level of gene expressions in each sample, we determined expected Fragments



Per Kilobase of transcript per Million mapped reads (FPKM) values which were substantially higher in both treatment groups as compared to the control group ([Supplementary Figure 6](#)).

Analysis of differential gene expression

DEGs between different groups

A total of 75,321 differentially expressed genes were annotated in all samples. In comparison with CK, a total of 37,395 DEGs of the B30_CK group were identified in which 34,436 genes were upregulated while 2,959 genes were downregulated. However, 22,288 DEGs were upregulated while 23,714 were downregulated between A26_CK and B30_CK treatment groups. Between A26_CK and CK groups there were only 879 genes downregulated while the remaining 49,136 were upregulated ([Figure 9A](#)).

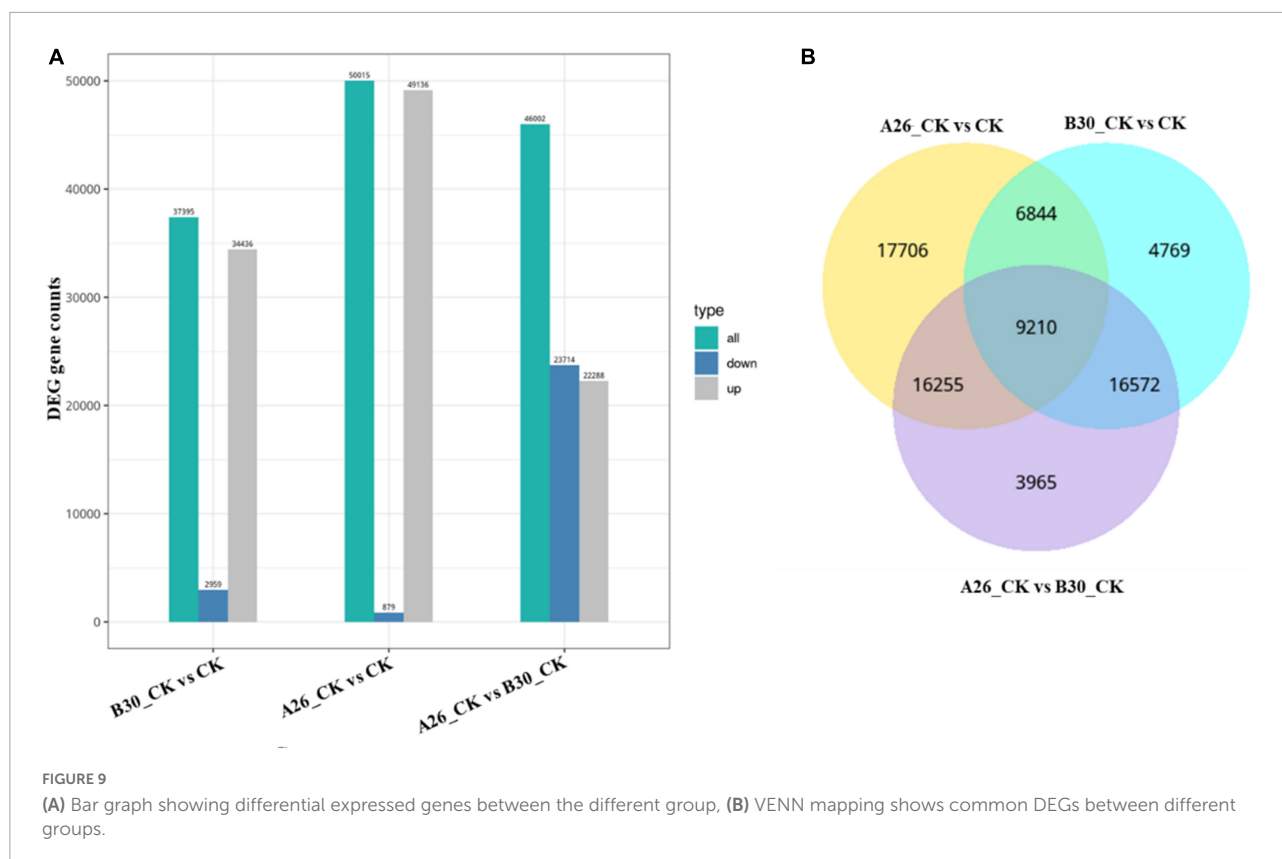
Common and unique DEGs among treatment groups

Venn diagram analysis showed that A26_CKvsCK shared 6844 common DEGs with B30_CKvsCK, and 16255 genes with

the A26_CKvsB30_CK group. While, 17706 DEGs were unique. Similarly, the A26_CKvsB30_CK group shared 16572 DEGs with B30_CKvsCK having 3965 DEGs unique. A total of 9,210 DEGs were common among all three groups ([Figure 9B](#)).

DEGs clustering and Kyoto encyclopedia of genes and genomes enrichment analysis

Heatmap cluster analysis of treatment groups exhibited significant differences in the gene expression ([Supplementary Figure 7](#)). Gene expression data from each sample were mapped to the KEGG pathway to determine involvement of DEGs in various classes of pathways. Using the R software package *enrichR*, we conducted pathway analysis and functional annotation for up and down-regulated genes. In B30_CK vs. CK group, a total of 37,395 DEGs were mapped to 347 KEGG pathways, out of which the top 20 enriched KEGG pathways are shown in [Figure 10A](#). Similarly, the top 20 enriched pathways of DEGs from A26_CK vs. CK and B30_CK vs. A26_CK are shown in [Figures 10B,C](#), respectively. Results revealed that DEGs were highly enriched in several pathways like protein processing in the endoplasmic reticulum, Ubiquitin mediated proteolysis,



Biosynthesis of amino acids, Endocytosis, Ribosome, and RNA transport ([Supplementary Table 7](#)).

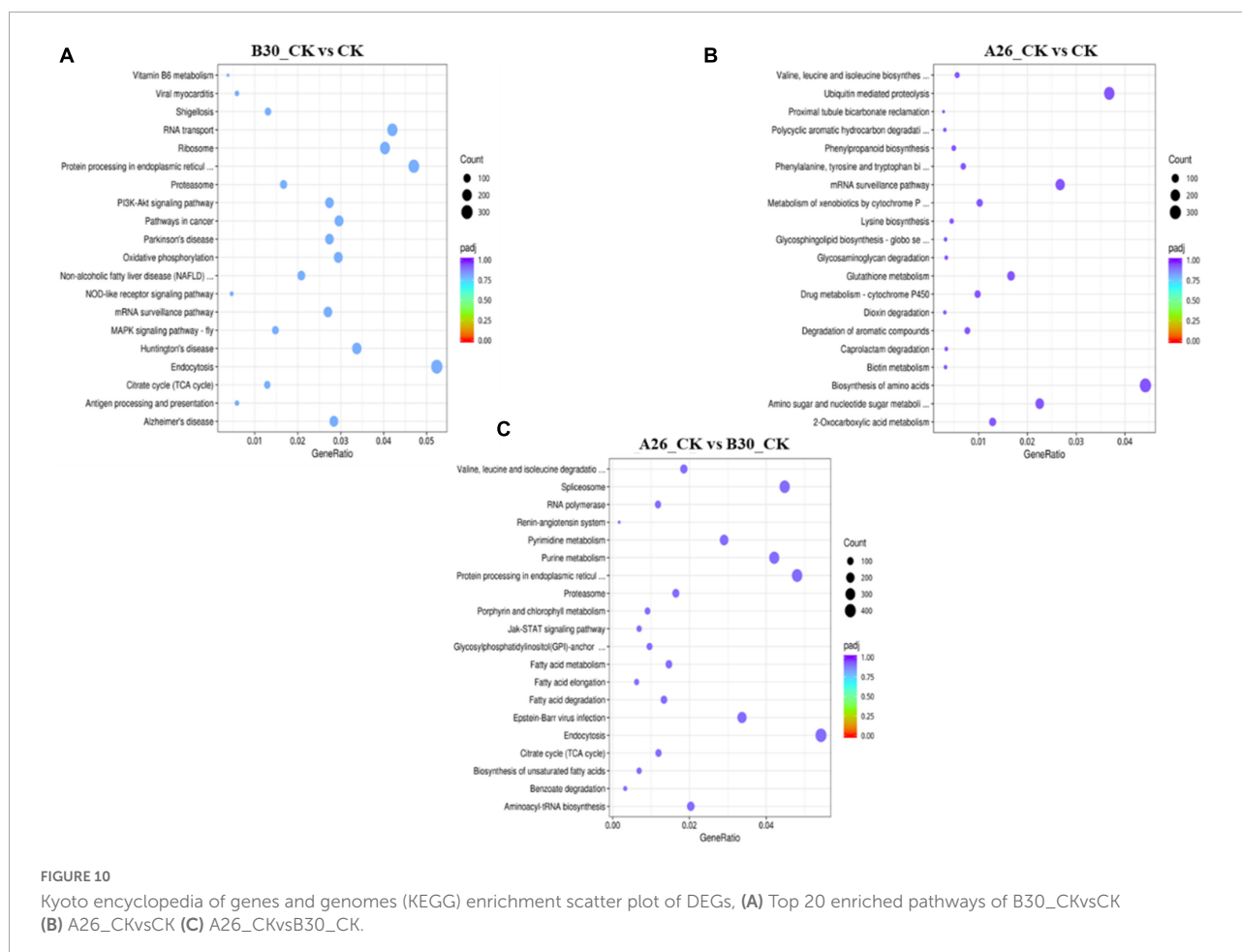
Discussion

In recent years, traditional Chinese medicine has gained much attention due to its benefits in preventing many diseases. Therefore, controlling the quality of Chinese herbal medicine is very crucial. *Asarum heterotropoides* Fr. Schmidt var. *mandshuricum* (Maxim.) Kitag is a valuable industrial and pharmaceutical plant that is used to cure a range of diseases ([Huang et al., 2003](#)). The roots or rhizome of the *Asarum* plant commonly known as Xixin in Chinese or Asari Radix et Rhizoma in the pharmaceutical industry is among the most prominent traditional Chinese herb ([Jing et al., 2017](#)). *S. asari* a pathogenic fungus infecting the Asarum plant is a growing concern. The biological treatment of phytopathogenic fungus *S. asari* is more efficient than chemical methods. For this purpose, Trichoderma strains have been used as a biocontrol agent because of their potential antifungal activity ([Gajera et al., 2013](#)).

In the present study, the plate confrontation method was used to check the antagonistic effect of two selected Trichoderma strains A26 (*T. hamatum*) and B30

(*T. koningiopsis*) against *S. asari*. Results indicated that both these strains exhibited the highest inhibition rates compared to the other strains. The morphological changes after the confrontation assay were also quite obvious. Previously, [Yuan et al. \(2017\)](#) reported the antimicrobial effect of *T. longibrachiatum* against *S. sclerotiorum* was highest compared to other pathogenic fungi including *Alternaria sclerotiorum* and *Rhizoctonia solani*. Moreover, *T. koningiopsis* has also shown a considerable inhibitory effect against *Sclerotinia*. Microscopic examination revealed that Trichoderma hyphae may grow alongside or penetrate and wrap around *S. sclerotiorum* hyphae, limiting their development and eventually causing *S. sclerotiorum* hyphae to disintegrate and damage ([Kang et al., 2017](#)). These findings clearly indicate the antagonistic activity and biocontrol mechanism of Trichoderma strains against phytopathogenic fungi.

Antifungal effects of metabolites produced by Trichoderma strains against *S. asari* were also investigated in the present study. Trichoderma produces a variety of secondary metabolites, including volatile and non-volatile compounds with potential antioxidant and antimicrobial activities ([El-Hasan et al., 2007](#)). The 6-pentyl-2H-pyran-2-one (6PP) is the only volatile metabolite, produced by different Trichoderma strains, which has been studied extensively with a major antagonistic activity against phytopathogens.



The 6PP has shown inhibitory effects against *Fusarium oxysporum*, *Rhizoctonia solani*, and *Fusarium moniliforme* (Serrano-Carreón et al., 2004; El-Hasan et al., 2007; Vos et al., 2015). In the present study, lower inhibition rate of volatile substances produced by *T. hamatum* A26 and *T. koningiopsis* B30 indicated the limited role of volatile metabolites of both strains in antifungal activity against phytopathogens.

In the present study, inhibitory effect of non-volatile metabolites produced by *T. hamatum* A26 was > 85% and it reached up to 100% for the B30 strain, indicating that non-volatile metabolites of both strains possess a potent antagonistic effect. These findings are in agreement with earlier studies reporting the antagonistic activity of two *Trichoderma* strains (*T. harzianum* and *T. brevis*) against four pathogens causing rice seedling blight (Zhan et al., 2020). Non-volatile metabolites exhibited higher inhibition rate against *F. graminearum* as compared to the inhibitory effect of volatile metabolites. These findings are in agreement with previous studies that also evidently revealed a stronger inhibitory effect of non-volatile metabolites against phytopathogens than volatile metabolites (Tapwal et al., 2011; Khaledi and Taheri, 2016; Zhao et al., 2020).

In the current study, LC-MS analysis was carried out to screen differential metabolites from A26 and B30 strains. Analysis of antifungal activity revealed that seven out of 14 metabolites exhibited the highest antifungal activity against *S. asari*. These metabolites are well-known for their antibacterial and antifungal properties (Tan et al., 2021). Eplerenone has been identified as a novel antibacterial substance for drug repurposing against multi-drug resistant bacteria (Asghar et al., 2021). Moreover, Behenic acid has also shown bactericidal activity against *Agrobacterium tumefaciens* T-37 and *Ralstonia solanacearum* RS-2 (Xie et al., 2021). Similarly, antimicrobial and antifungal activities of other abundant metabolites, Josamycin, methyleugenol, erythromycin, and minocycline, identified in the present study have also been reported earlier (Anzaku et al., 2017; Dekhnic et al., 2018; Garcia-Jimenez et al., 2018; Keman and Soyer, 2019; Mohammed Ali Al-Harrasi et al., 2021).

In the present study, KEGG classification of differential metabolites showed that enriched metabolites mainly included; alkaloids and derivatives, lipids and lipid-like molecules, phenylpropanoids and polyketides, organic acids and derivatives, benzenoids, oxygen like nitrogen compounds,

and organic oxygen compounds. These metabolites were involved in many metabolic pathways like tyrosine metabolism, phenylalanine metabolism, valine, leucine, and isoleucine biosynthesis, and pyrimidine metabolism. Metabolites present in tyrosine and phenylalanine metabolism pathways were upregulated indicating that these metabolites are necessary for the synthesis of many proteins involved in the development and growth. On the other hand, purine metabolism, lysine degradation, and taste transduction pathways were downregulated and only a few metabolites were identified in these pathways. Previous studies have shown that secondary metabolites synthesized by non-pathogenic fungal strains were converted into antifungal substances of several types, contributing to antifungal action (Strobel, 2003). Secondary metabolite synthesis (particularly phytoalexins) was found to be an essential plant defensive mechanism against plant diseases (Yuan et al., 2019). Antimicrobial phenolics such as lignins, coumarins, flavonoids, and isoflavonoids are formed from phenylpropanoid molecules. These metabolites are produced in response to microbial invasion and can stop the proliferation of infections (Harman et al., 2004; Huang et al., 2010).

In the present study, the activity of antioxidant enzymes like SOD, POD, CAT, and MDA was also determined to evaluate the effect of treatment (with *Trichoderma* strains) on antioxidant defense of *S. asari*. Lipid peroxidation refers to the interaction of reactive oxygen species (ROS) with lipids. MDA is a product of lipid peroxidation and a high level of MDA is an indicator of the damaged cell membrane (Morales and Munné-Bosch, 2019). SOD enzyme scavenges free oxygen radicals (O^{-2}) into hydrogen peroxide H_2O_2 , while, POD and CAT effectively remove H_2O_2 from the cell and maintain the active oxygen production in the cell (Inze, 2001; Schopfer et al., 2001; Liu et al., 2014). Libin et al. (2013) reported that the ethyl acetate extract of *Trichoderma harzianum* fermentation broth can reduce the content of soluble protein of *Phytophthora infestans*, while reducing the activity of bacterial protective enzymes (SOD, CAT, and POD), and increasing the MDA content in the bacterial body (Libin et al., 2013). Xun et al. (2013) observed that the ethyl acetate extract of strain T-43 fermentation broth has a significant effect on the main antioxidant enzymes (SOD, POD, CAT, and PPO) of pathogenic bacteria (Xun et al., 2013). This extract inhibited the growth of pathogenic bacteria by destroying the defense system of pathogenic bacteria. In the present study, MDA content was increased continuously upon treatment with antagonistic strains as compared to the control group. Similarly, the activities of antioxidant enzymes (SOD, POD, and CAT) in *S. asari* were significantly lower when treated with antagonist *Trichoderma* strains (A26 and B30) indicating their effectiveness against the *Sclerotinia* disease of *Asarum*.

In the present study, transcriptome analysis was also carried out to identify differential genes involved in biological pathways. Differentially expressed genes were identified according to the relative expression levels in different samples, and their

functional annotation and enrichment analysis were performed (Wang et al., 2009). Results of DEGs analysis showed that, many upregulated DEGs were related to pathways like protein processing in the endoplasmic reticulum, biosynthesis of amino acids, amino sugar and nucleotide sugar metabolism, endocytosis, ribosome, and RNA transport pathways. Amino acid biosynthesis and protein processing in the endoplasmic reticulum are major pathways that are necessary for the synthesis and transport of proteins (Yang et al., 2021).

Previous studies have reported that antagonistic activity of *Trichoderma* spp. stems from the expression of certain genes which regulate the secretion of enzymes like chitinases, cellulases, glucanases, and xylanases which can degrade cell wall (Harman et al., 2004). Some of the *Trichoderma* genes encoding enzymes have been discovered to indirectly induce plant resistance (Bolar et al., 2000). Furthermore, the presence of *Trichoderma* has also shown to stimulate the expression of plant chitinases (Shoresh and Harman, 2010). Moreover, significantly higher enzymatic activity of β -1,3-glucanase and chitinases in postharvest anthracnose of chili pepper was observed after treatment with *T. koningiopsis*, than the control group in a previous study (Ruangwong et al., 2021).

Overall findings of the present study indicated the importance of enriched metabolic networks particularly protein synthesis and signal transduction pathways in the biocontrol mechanism of *T. koningiopsis* B30 and *T. hamatum* A26 strains against *S. asari*. Therefore, it might be a promising strategy by applying biological treatment using *Trichoderma* strains, *T. koningiopsis* B30, and *T. hamatum* A26 as antagonist against *Asarum sclerotiorum*. Our findings also provide practical insights about inhibition of fungal phytopathogens with non-volatile compounds and their potential use a green strategy to control crop pests.

Conclusion

The present study concluded that treatment with *Trichoderma* substantially damaged the antioxidant defense of *S. asari* by decreasing the activities of its protective enzymes (POD, SOD, and CAT) while increasing MDA activity. Furthermore, non-volatile compounds of *Trichoderma* (Abamectin, Eplerenone, Behenic acid, Josamycin, Erythromycin, Methyleugenol, and Minocycline) showed promising antifungal activity for the inhibition of *S. asari*. Findings of the present study indicated that *T. Koningiopsis* B30, and *T. hamatum* A26 could be used as biocontrol agents for the treatment of *Asarum Sclerotiorum*. Moreover, our findings provided molecular insights about the metabolic pathways responsible for the production of antifungal metabolites which can effectively inhibit the growth of *S. asari* and save the plant from fungal diseases.

Data availability statement

The datasets presented in this study can be found in NCBI SRA under the project number PRJNA820374 (<https://www.ncbi.nlm.nih.gov/bioproject/?term=PRJNA820374>).

Author contributions

ZhW designed the experiment, methodology, conducted the experiment, analyzed the data, and wrote the manuscript. ZhW, XQ, and ZZ performed the experiment and analyzed the data. BL performed the methodology. GZ supervised and revised the draft. WL contributed to project administration. YT contributed to writing—review and editing. All authors have read and approved the final version of this manuscript.

Funding

This study was funded by Science and Technology Department Project from Jilin Province of China (20190304017YY) and National key research special project of China (2019YFC1710700).

References

- Anzaku, A. A., Akyala, J. I., Juliet, A., and Obianuju, E. C. (2017). Antibacterial activity of lauric acid on some selected clinical isolates. *Ann. Clin. Lab. Res.* 5:170. doi: 10.21767/2386-5180.1000170
- Asghar, A., Tan, Y.-C., Shahid, M., Yow, Y.-Y., and Lahiri, C. (2021). Metabolite profiling of Malaysian *Gracilaria Edulis* reveals eplerenone as novel antibacterial compound for drug repurposing against MDR bacteria. *Front. Microbiol.* 12:653562. doi: 10.3389/fmicb.2021.653562
- Benítez, T., Rincón, A. M., Limón, M. C., and Codon, A. C. (2004). Biocontrol mechanisms of *Trichoderma* strains. *Int. Microbiol.* 7, 249–260.
- Blaženović, I., Kind, T., Ji, J., and Fiehn, O. (2018). Software tools and approaches for compound identification of LC-MS/MS data in metabolomics. *Metabolites* 8:31. doi: 10.3390/metabo8020031
- Bolar, J. P., Norelli, J. L., Wong, K.-W., Hayes, C. K., Harman, G. E., and Aldwinckle, H. S. (2000). Expression of endochitinase from *Trichoderma Harzianum* in transgenic apple increases resistance to apple scab and reduces vigor. *Phytopathology* 90, 72–77. doi: 10.1094/PHYTO.2000.90.1.72
- Bolton, M. D., Thomma, B. P. H. J., and Nelson, B. D. (2006). *Sclerotinia Sclerotiorum* (Lib.) de Bary: biology and molecular traits of a cosmopolitan pathogen. *Mol. Plant Pathol.* 7, 1–16. doi: 10.1111/j.1364-3703.2005.00316.x
- Caporaso, J. G., Lauber, C. L., Walters, W. A., Berg-Lyons, D., Huntley, J., Fierer, N., et al. (2012). Ultra-High-throughput microbial community analysis on the illumina HiSeq and MiSeq platforms. *ISME J.* 6, 1621–1624. doi: 10.1038/ismej.2012.8
- Conesa, A., Götz, S., García-Gómez, J. M., Terol, J., Talón, M., and Robles, M. (2005). Blast2GO: a universal tool for annotation. Visualization and analysis in functional genomics research. *Bioinformatics* 21, 3674–3676. doi: 10.1093/bioinformatics/bti610
- Dan, Y., Liu, H.-Y., Gao, W.-W., and Chen, S.-L. (2010). Activities of essential oils from *Asarum Heterotropoides* Var. *Mandshuricum* against five phytopathogens. *Crop. Prot.* 29, 295–299. doi: 10.1016/j.cropro.2009.12.007
- Dekhnich, N. N., Ivanchik, N. V., and Kozlov, R. S. (2018). Comparison of in vitro activity of various macrolides against *Helicobacter Pylori*. *Clin. Microbiol. Antimicrob. Chemother.* 20, 192–197. doi: 10.36488/cm.2018.3.192-197
- El-Hasan, A., Walker, F., Schöne, J., and Buchenauer, H. (2007). Antagonistic effect of 6-Pentyl-alpha-pyrone produced by *Trichoderma Harzianum* toward *Fusarium Moniliforme*. *J. Plant Dis. Prot.* 114, 62–68. doi: 10.1007/BF03356205
- Finn, R. D., Clements, J., and Eddy, S. R. (2011). HMMER web server: interactive sequence similarity searching. *Nucleic Acids Res.* 39, W29–W37. doi: 10.1093/nar/gkr367
- Gajera, H., Domadiya, R., Patel, S., Kapopara, M., and Golakiya, B. (2013). Molecular mechanism of *Trichoderma* as bio-control agents against phytopathogen system—a review. *Curr. Res. Microbiol. Biotechnol.* 1, 133–142.
- García-Jimenez, A., García-Molina, F., Teruel-Puche, J. A., Saura-Sanmartin, A., García-Ruiz, P. A., Ortiz-Lopez, A., et al. (2018). Catalysis and inhibition of *Tyrosinase* in the presence of cinnamic acid and some of its derivatives. *Int. J. Biol. Macromol.* 119, 548–554. doi: 10.1016/j.ijbiomac.2018.07.173
- Gil, S. V., Pastor, S., and March, G. J. (2009). Quantitative isolation of biocontrol agents *Trichoderma Spp.*, *Gliocladium Spp.* and actinomycetes from soil with culture media. *Microbiol. Res.* 164, 196–205. doi: 10.1016/j.micres.2006.11.022
- Harman, G. E., Howell, C. R., Viterbo, A., Chet, I., and Lorito, M. (2004). *Trichoderma* Species-opportunistic, avirulent plant symbionts. *Nat. Rev. Microbiol.* 2, 43–56. doi: 10.1038/nrmicro797
- Huang, J., Gu, M., Lai, Z., Fan, B., Shi, K., Zhou, Y.-H., et al. (2010). Functional analysis of the *Arabidopsis* PAL gene family in plant growth, development, and response to environmental stress. *Plant Physiol.* 153, 1526–1538. doi: 10.1104/pp.110.157370
- Huang, S. M., Kelly, L. M., and Gilbert, M. G. (2003). “Aristolochiaceae,” in *Flora of China*, Vol. 5, eds C. Y. Wu and P. H. Raven (Beijing: Science Press)
- Inze, D. (2001). *Oxidative Stress in Plants*. Boca Raton, FL: CRC Press.
- Jing, Y., Zhang, Y.-F., Shang, M.-Y., Liu, G.-X., Li, Y.-L., Wang, X., et al. (2017). Chemical constituents from the roots and rhizomes of *Asarum Heterotropoides*

Conflict of interest

The authors declare that the research was conducted in the absence of any commercial or financial relationships that could be construed as a potential conflict of interest.

Publisher's note

All claims expressed in this article are solely those of the authors and do not necessarily represent those of their affiliated organizations, or those of the publisher, the editors and the reviewers. Any product that may be evaluated in this article, or claim that may be made by its manufacturer, is not guaranteed or endorsed by the publisher.

Supplementary material

The Supplementary Material for this article can be found online at: <https://www.frontiersin.org/articles/10.3389/fmicb.2022.997050/full#supplementary-material>

- Var. *Mandshuricum* and the in vitro anti-inflammatory activity. *Molecules* 22:125. doi: 10.3390/molecules22010125
- Kalia, A., and Gosal, S. K. (2011). Effect of pesticide application on soil microorganisms. *Arch. Agron. Soil Sci.* 57, 569–596. doi: 10.1080/03650341003787582
- Kang, Y., Yan, L., Lei, Y., Wan, L., Huai, D., Wang, Z., et al. (2017). Biocontrol mechanism of *Trichoderma pseudocanning* against peanut sclerotinia. *Chin. J. Oil Crops* 39:842.
- Keman, D., and Soyer, F. (2019). Antibiotic-Resistant *Staphylococcus Aureus* Does not develop resistance to vanillic acid and 2-hydroxycinnamic acid after continuous exposure in vitro. *ACS Omega* 4, 15393–15400. doi: 10.1021/acsomega.9b01336
- Khaledi, N., and Taheri, P. (2016). Biocontrol mechanisms of *Trichoderma Harzianum* against soybean charcoal rot caused by *Macrophomina Phaseolina*. *J. Plant Prot. Res* 56, 21–36. doi: 10.1515/jppr-2016-0004
- Kim, T. G., and Knudsen, G. R. (2008). Quantitative real-time PCR effectively detects and quantifies colonization of sclerotia of *Sclerotinia Sclerotiorum* by *Trichoderma Spp.* *Appl. Soil Ecol.* 40, 100–108. doi: 10.1016/j.apsoil.2008.03.013
- Küçük, Ç., and Kivanç, M. (2005). In vitro antifungal activity of strains of *Trichoderma Harzianum*. *Turkish J. Biol.* 28, 111–115.
- Li, B., and Dewey, C. N. (2011). RSEM: accurate transcript quantification from RNA-Seq data with or without a reference genome. *BMC Bioinformatics* 12:323. doi: 10.1186/1471-2105-12-323
- Libin, Y., Ruiqing, S., and Chongwei, L. (2013). Effect of ethyl acetate extract of *Trichoderma harzianum* fermentation broth on physiological indicators of *Phytophthora infestans*. *J. Beijing For. Univ.* 35, 92–96.
- Ling, L., Wensong, S., Tianjing, Z., Baoyu, S., and Ying, L. (2021). Identification and biological characterization of antagonistic antibacterial antibacterial antibiotics for *Asarum Sclerotiorum* liao. *J. Sichuan Agric. Univ.* 38, 558–563.
- Liu, N., Lin, Z., Guan, L., Gaughan, G., and Lin, G. (2014). Antioxidant enzymes regulate reactive oxygen species during pod elongation in *Pisum Sativum* and *Brassica Chinensis*. *PLoS One* 9:e87588. doi: 10.1371/journal.pone.0087588
- Manzinger, L., Antal, Z., and Kredics, L. (2002). Ecophysiology and breeding of *Mycoparasitic Trichoderma* strains. *Acta Microbiol. Immunol. Hung.* 49, 1–14. doi: 10.1556/amicro.49.2002.1.1
- Martin, M. (2011). Cutadapt removes adapter sequences from high-throughput sequencing reads. *EMBnet. J.* 17, 10–12. doi: 10.14806/ej.17.1.200
- Mayo-Prieto, S., Campelo, M. P., Lorenzana, A., Rodríguez-González, A., Reinoso, B., Gutiérrez, S., et al. (2020). Antifungal activity and bean growth promotion of *Trichoderma* strains isolated from seed vs soil. *Eur. J. Plant Pathol.* 158, 817–828. doi: 10.1007/s10658-020-02069-8
- Mohammed Ali Al-Harrasi, M., Mohammed Al-Sadi, A., Al-Tamimi, A. M., Al-Sabahi, J. N., and Velazhahan, R. (2021). In vitro production of antifungal phenolic acids by *Hypomyces Perniciosus*, the causal agent of wet bubble disease of *Agaricus Bisporus*. *All Life* 14, 948–953. doi: 10.1080/26895293.2021.1987340
- Möller, E. M., Bahnweg, G., Sandermann, H., and Geiger, H. H. A. (1992). Simple and efficient protocol for isolation of high molecular weight DNA from *Filamentous Fungi*, fruit bodies, and infected plant tissues. *Nucleic Acids Res.* 20:6115.
- Monte, E. (2001). Understanding *Trichoderma*: between biotechnology and microbial ecology. *Int. Microbiol.* 4, 1–4.
- Morales, M., and Munné-Bosch, S. (2019). Malondialdehyde: facts and artifacts. *Plant Physiol.* 180, 1246–1250. doi: 10.1104/pp.19.00405
- Perumalsamy, H., Chang, K. S., Park, C., and Ahn, Y.-J. (2010). Larvicidal activity of *Asarum Heterotropoides* root constituents against insecticide-susceptible and -resistant *Culex Pipiens* Fallens and *Aedes Aegypti* and *Ochlerotatus Togo*. *J. Agric. Food Chem.* 58, 10001–10006. doi: 10.1021/jf102193k
- Ruangwong, O.-U., Pornsuriya, C., Pitija, K., and Sunpapao, A. (2021). Biocontrol mechanisms of *Trichoderma Koningiopsis* PSU3-2 against postharvest anthracnose of chili pepper. *J. Fungi* 7:276. doi: 10.3390/jof7040276
- Schopfer, P., Plachy, C., and Frahy, G. (2001). Release of reactive oxygen intermediates (superoxide radicals, hydrogen peroxide, and hydroxyl radicals) and peroxidase in germinating radish seeds controlled by light, gibberellin, and abscisic acid. *Plant Physiol.* 125, 1591–1602. doi: 10.1104/pp.125.4.1591
- Serrano-Carreón, L., Flores, C., Rodríguez, B., and Galindo, E. (2004). *Rhizoctonia Solani*, an Elicitor of 6-Pentyl- α -pyrone production by *Trichoderma Harzianum* in a two liquid phases, extractive fermentation system. *Biotechnol. Lett.* 26, 1403–1406. doi: 10.1023/B:BILE.0000045640.71840.b5
- Sharma, P., Kumar, V., Ramesh, R., Saravanan, K., Deep, S., Sharma, M., et al. (2011). Biocontrol genes from *Trichoderma* species: a review. *Afr. J. Biotechnol.* 10, 19898–19907. doi: 10.5897/AJBX11.041
- Shentu, X.-P., Liu, W.-P., Zhan, X.-H., Xu, Y.-P., Xu, J.-F., Yu, X.-P., et al. (2014). Transcriptome sequencing and gene expression analysis of *Trichoderma Brevicompactum* under different culture conditions. *PLoS One* 9:e94203. doi: 10.1371/journal.pone.0094203
- Shoresh, M., and Harman, G. E. (2010). Differential expression of maize chitinases in the presence or absence of *Trichoderma Harzianum* strain T22 and indications of a novel exo-endo-heterodimeric chitinase activity. *BMC Plant Biol.* 10:136. doi: 10.1186/1471-2229-10-136
- Strobel, G. A. (2003). Endophytes as sources of bioactive products. *Microbes Infect.* 5, 535–544. doi: 10.1016/S1286-4579(03)00073-X
- Tamura, K., Stecher, G., and Kumar, S. (2021). MEGA11: molecular evolutionary genetics analysis version 11. *Mol. Biol. Evol.* 38, 3022–3027. doi: 10.1093/molbev/msab120
- Tan, J., Jiang, S., Tan, L., Shi, H., Yang, L., Sun, Y., et al. (2021). Antifungal activity of minocycline and azoles against fluconazole-resistant candida species. *Front. Microbiol.* 12:1185. doi: 10.3389/fmicb.2021.649026
- Tapwal, A., Garg, S., Gautam, N., and Kumar, R. (2011). In vitro antifungal potency of plant extracts against five phytopathogens. *Braz. Arch. Biol. Technol.* 54, 1093–1098. doi: 10.1590/S1516-89132011000600003
- Tjamos, E. C., Papavizas, G. C., and Cook, R. J. (2013). *Biological Control of Plant Diseases: Progress and Challenges for the Future*, Vol. 230. Berlin: Springer Science & Business Media.
- Tyagi, S., Lee, K.-J., Shukla, P., and Chae, J.-C. (2020). Dimethyl disulfide exerts antifungal activity against sclerotinia minor by damaging its membrane and induces systemic resistance in host plants. *Sci. Rep.* 10:6547. doi: 10.1038/s41598-020-63382-0
- Vos, C. M. F., De Cremer, K., Cammue, B. P. A., and De Coninck, B. (2015). The toolbox of *Trichoderma Spp.* in the biocontrol of *Botrytis Cinerea* disease. *Mol. Plant Pathol.* 16, 400–412. doi: 10.1111/mpp.12189
- Wang, C., and Wu, Y. (1982). Study on *Sclerotinia Asari* I. Loss investigation, symptom types and pathogens. *J. Shenyang Agric. Univ.* 2, 52–61.
- Wang, C., and Wu, Y. (1983). Research on *Sclerotinia Asari* - II. Law of infection and incidence. *J. Shenyang Agric. Univ.* 2, 71–83.
- Wang, C., and Wu, Y. (1984). Occurrence and control of *Asarum sclerotiorum*. *New Agric.* 12, 20–21.
- Wang, Z., Gerstein, M., and Snyder, M. R. N. A. (2009). Seq: a revolutionary tool for transcriptomics. *Nat. Rev. Genet.* 10, 57–63. doi: 10.1038/nrg2484
- White, T. J., Bruns, T., Lee, S., and Taylor, J. (1990). Amplification and direct sequencing of fungal ribosomal RNA genes for phylogenetics. *PCR Protoc.* 18, 315–322. doi: 10.1016/B978-0-12-372180-8.50042-1
- Xie, Y., Peng, Q., Ji, Y., Xie, A., Yang, L., Mu, S., et al. (2021). Isolation and identification of antibacterial bioactive compounds from *Bacillus Megaterium* L2. *Front. Microbiol.* 12:645484. doi: 10.3389/fmicb.2021.645484
- Xun, D., Ruiqing, S., Xiaoshuang, S., and Dachuan, Y. (2013). Inhibitory mechanism of high-efficiency *Trichoderma* strain on *Pinus sylvestris* blight disease. *J. Cent. South Univ. For. Technol.* 32, 21–27.
- Yang, Y., He, Y., Jin, Y., Wu, G., and Wu, Z. (2021). “Amino Acids in Endoplasmic Reticulum Stress and Redox Signaling,” in *Amino Acids in Nutrition and Health*, ed. G. Wu (Berlin: Springer), 35–49. doi: 10.1007/978-3-030-74180-8_3
- Yuan, C., Yang, X., Jiang, C., Yao, Z., Jia, R., Ren, L., et al. (2017). A *Trichoderma longbranchus* that can antagonize three soil-borne disease pathogenic fungi. *Herbol. Sci.* 34, 246–254.
- Yuan, M., Huang, Y., Ge, W., Jia, Z., Song, S., Zhang, L., et al. (2019). Involvement of jasmonic acid, ethylene and salicylic acid signaling pathways behind the systemic resistance induced by *Trichoderma Longibrachiatum* H9 in cucumber. *BMC Genomics* 20:144. doi: 10.1186/s12864-019-5513-8
- Zeki, Ö.C., Eylem, C. C., Reçber, T., Kir, S., and Nemitlu, E. (2020). Integration of GC-MS and LC-MS for untargeted metabolomics profiling. *J. Pharm. Biomed. Anal.* 190:113509. doi: 10.1016/j.jpba.2020.113509
- Zeng, H., Jin, Y., Bao, L., and Wang, P. (2004). Analysis on fingerprint chromatogram of the volatile oils obtained from *Asarum Heterotropoides* with different methods. *J. Test Meas. Technol.* 18, 232–236.
- Zhan, X., Tai, L., Liu, T., Zhang, L., Zheng, W., and Jin, Y. (2020). Study on the antagonistic effects of two *Trichoderma* species on the pathogenic bacterial blight of rice in cold regions. *China Rice* 26:96.
- Zhao, D., He, H., Wu, S., Chen, X., Tan, Q., and Yang, X. (2020). Biocontrol mechanism of *Trichoderma aculeatus* GYSW-6m1 on strawberry anthracnose and its role in preventing and promoting growth. *Chin. J. Biol. Control* 36:587.